



Mapping the Mechanical Properties of Cement-based Materials By Using CSM and Ultra-fast Nanoindentation

Application Note

M. Sebastiani

University of Rome "ROMA TRE", Mechanical and Industrial Engineering Department,
Via della della Vasca Navale 79, 00146 Rome, Italy

Introduction

Cement-based composites still represent the most used materials in the construction industry, due to their low production and processing costs.

Nonetheless, the fundamental mechanisms underlying the microstructure build-up and the in-service mechanical behaviour are still mostly unknown, due to the extreme complexity of such materials [1].

Cement-based composites have been already identified as nano-granular multi-scaled materials, with a strong heterogeneity that manifests itself at multiple scales, in form of multiple pore spaces and multiple minerals that build-up the solid phase.

Such complexity is further increased by the recent growing use of nano-additives in cements [2], which often involves the formation of nano-phases that are not fully characterised, yet.

The primary hydration product of cement pastes and concrete is the calcium-silicate-hydrate (CSH), which act as the main binding phase and mostly influences the mechanical and creep properties of the system [1].

Recent studies [3–5] have also confirmed the presence of different solid phases in a cement-based composite: (a) mortar-concrete ($>10^{-3}$ m), (b) cement paste ($<10^{-4}$ m), (c) C-S-H matrix ($<10^{-6}$ m) and (d) CSH solid phase (10^{-9} - 10^{-10} m).

The elementary C-S-H particle is a nanoparticle of the average dimension of the order of 5 nm, which includes an average nanoporosity of 18%. The presence of "structural water" at the nano-scale gives relevant time-dependent mechanical properties to these materials. Depending on the level of packing of the elementary building block, high-density (HD) and low-density CSH phases have been recently proposed as possible hydrated mechanical phases in cement. Tailoring of such phases is the key-issue for a proper control of the in-service behaviour of such materials.

In this study, we propose to investigate the nano-mechanical properties of a commercial cement paste by the use of an improved statistical nanoindentation method.

This technique, which was originally proposed in 2004 [3], is based on the realization of grids of hundreds of nanoindentation tests, coupled with



Agilent Technologies

a statistical analysis (deconvolution) for the identification of the different mechanical phases and their distribution over the sampled area.

The principle of statistical nanoindentation is described in Figure 1a-b. If we assume that the distribution of the elastic modulus (E) is well approximated by a Gaussian distribution, then the average property of each phase can be analytically obtained, for a multi-phase material, by fitting the experimental frequency distribution of the mechanical property with the theoretical probability density function (PDF), as schematically shown in the Figure 1b. It is clear from Figure 1b that only those phases whose peak intensity is much higher than the background noise will be detected in a statistically consistent way. Starting from the original idea, the method has been further implemented and optimised in the last ten years by a number of research groups [4–23].

LD and HD CSH phases in cement pastes have been recently identified by the use of this method and the analysis of the elastic modulus maps [6–8]. Recent papers also showed that fitting of the cumulative distribution functions (CDF) is statistically more reliable, in comparison with the PDF, because CDF analysis does not require the choice of a bin-size to build the frequency histogram.

However, strong limitations are still present, due to the relatively low number of tests that can be realized using a conventional nanoindentation approach in a reasonable amount of time. This is absolutely not sufficient to make quantitative and reliable analysis of secondary phases (e.g. the HD-CSH and the unhydrated clinker phases), whose peak intensity is usually of the same order of the typical noise associated to the experiments.

To solve this issue, we propose the use of the Agilent's Express Test option in order to dramatically improve the statistical

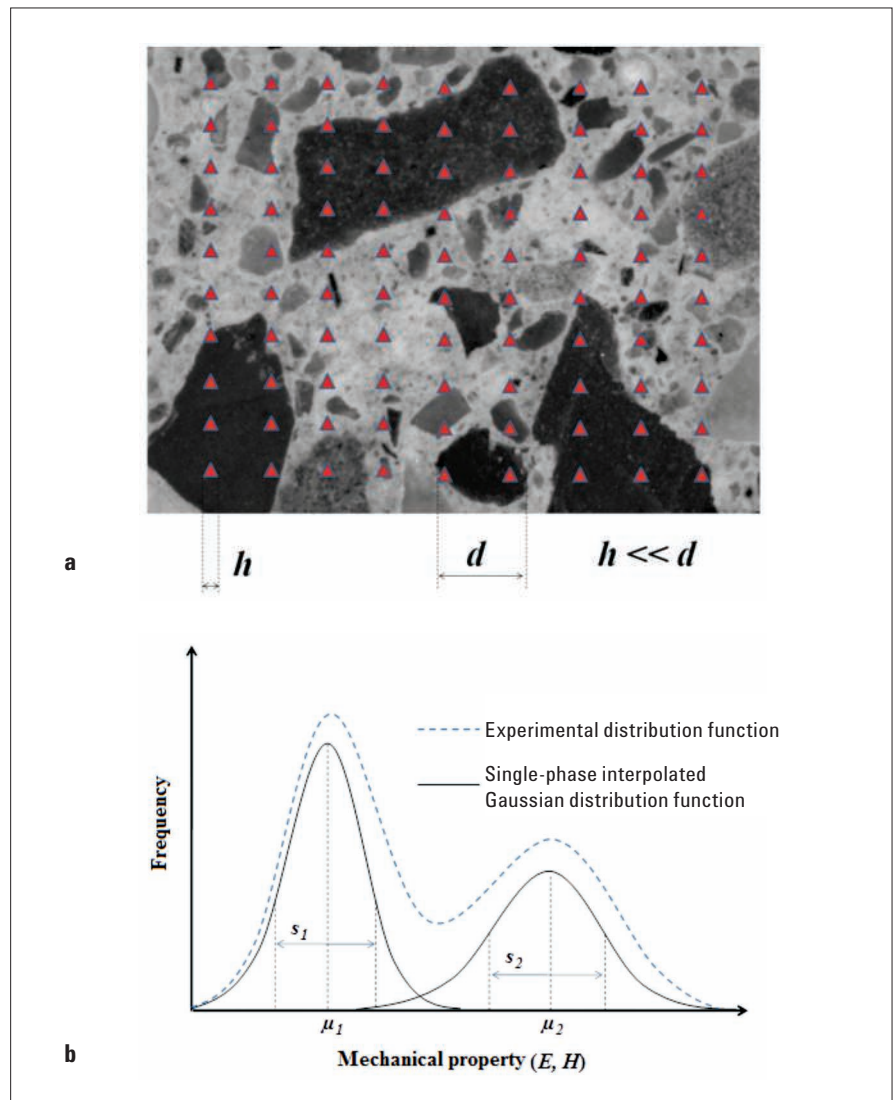


Figure 1. Concept of statistical nanoindentation to map the mechanical properties of multi-phase materials. (a) a grid of tests is performed and (b) the frequency distribution plot of obtained properties (Elastic modulus and/or hardness) are analyzed through deconvolution processes, in order to identify mechanical phases.

reliability and spatial resolution of mechanical properties mapping by nanoindentation. This target is achieved by the realization of more than 30000 valid tests in less than 10 hours on a commercial cement paste.

The maps obtained by using both the Express Test and the conventional Continuous Stiffness Measurement

(CSM) approaches are compared with SEM-EDS microstructural observations of the same areas of the tests.

The final purpose of this work was to assess the correlation between hydration mechanisms and mechanical properties of the basic constituents of cement, by using a nanoindentation based approach, coupled with SEM-EDS mapping.

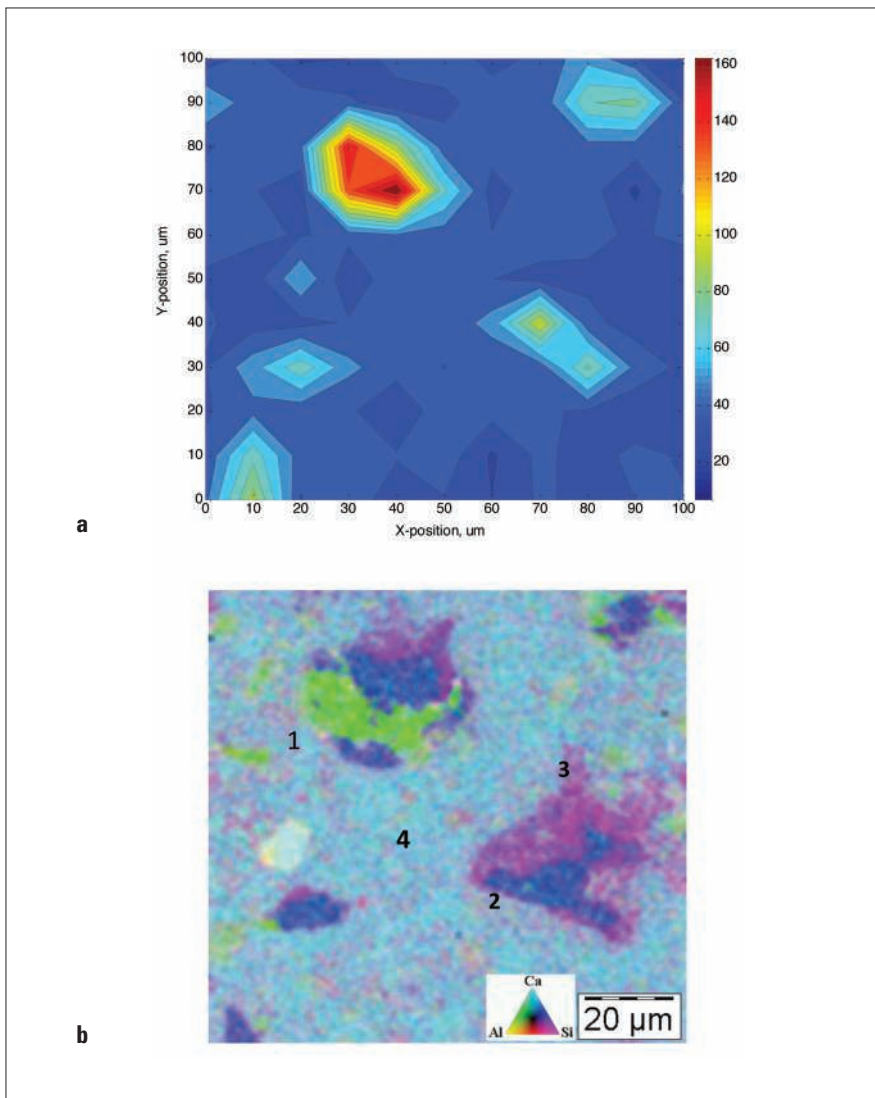


Figure 2. (a) Elastic modulus map (GPa), as obtained by the conventional CSM ($10 \times 10 = 100$ indents matrix, spacing $10 \mu\text{m}$, indentation depth 100 nm). (b) SEM-EDS map of the same area, where the green phase corresponds to C4AF clinker phases (label 1), the blue one to C3S clinker phase (label 2), the violet and light-blue to the HD and LD CSH, labels 3 and 4 respectively.

Experimental Details

Cement paste samples were produced from a commercial CEM I 52.5R Portland cement, using a w/b ratio of 0.36. After a curing time of 28 days under 100% humidity environment, samples were polished down to a surface roughness $R_a < 20 \text{ nm}$.

Nanoindentation tests are performed with an Agilent G200 NanoIndenter having CSM and Express Test, which includes NanoVision and a DCM II fitted with a Berkovich indenter. The standard material is fused silica.

In case of CSM tests, a grid of 20×20 indents was realized over a squared area

of $200 \times 200 \mu\text{m}^2$, with a spacing of $10 \mu\text{m}$ and a maximum indentation depth of 100 nm . CSM tests were useful to identify the best penetration gives which reduces both the effect of surface roughness (more evident at shallower depths) and the ones due to porosity (more important at larger depths) on the modulus vs depth profile: 100 nm was found to be the optimal depth giving the most reliable evaluation of elastic modulus for such materials.

Ultra-fast tests were performed by prescribing arrays of 50×50 indents over an area of $100 \times 100 \mu\text{m}^2$, by fixing a maximum depth of 100 nm and a spacing of $2 \mu\text{m}$.

Express Test performs one complete indentation cycle per second, including approach, contact detection, load, unload, and movement to the next indentation site. In this way, quantitative maps of both the elastic modulus and the hardness of a surface can be realized in a reasonable time.

In this work, Fifteen different matrices were performed in a single day of testing (ten hours), being the overall number of performed tests equal to 37500.

Detailed microstructural and compositional observation of the same areas of the tests were finally performed by SEM-EDS analysis.

Results and Discussion

Figure 2 shows an optical micrograph where eight different maps (squared areas in dark grey) obtained by ultra-fast nanoindentation can be compared with the one obtained by conventional CSM nanoindentation (letter "A").

The elastic modulus maps obtained by both the conventional nanoindentation and the Express Test are reported in the Figures 3a and 4a, respectively. The corresponding SEM-EDS maps are also reported in the Figures 3b and 4b.

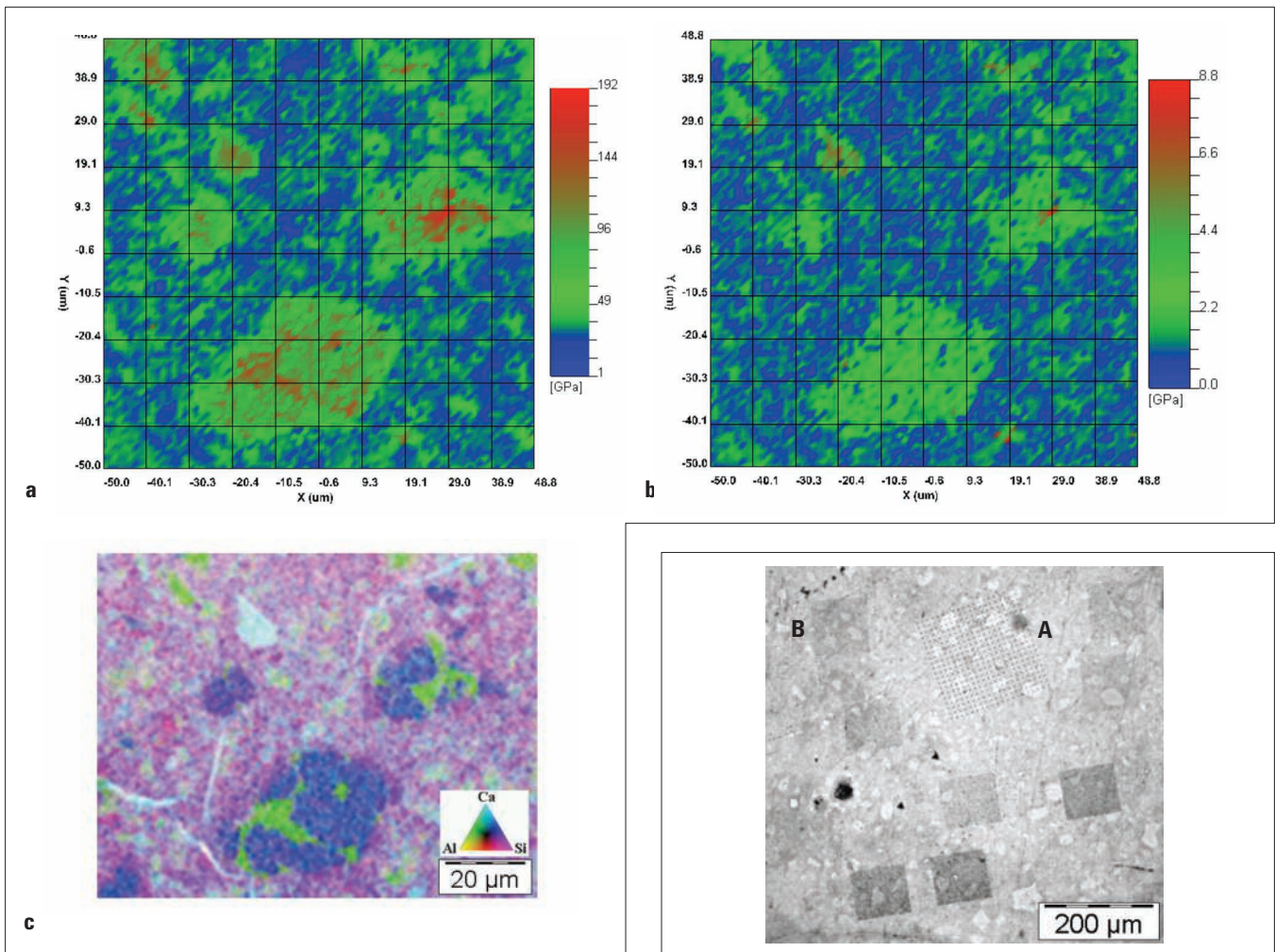


Figure 3. (a) Elastic modulus map (GPa), as obtained by the express test (50x50=2500 indents matrix, spacing 2µm, indentation depth 100 nm). (b) Hardness map (GPa) from the same test. (c) SEM-EDS map of the same area, where the orange phase corresponds to C4AF clinker phases, the light-blue to C3S clinker phase.

Figure 4. Optical micrograph where eight different maps (squared areas in dark grey) obtained by ultra-fast nanoindentation can be compared with the one obtained by conventional CSM nanoindentation (label "A"). Results of map "B" are those reported in the Figure 3a–c.

In both cases, a good correspondence between the elastic modulus maps and the SEM-EDS observations is observed.

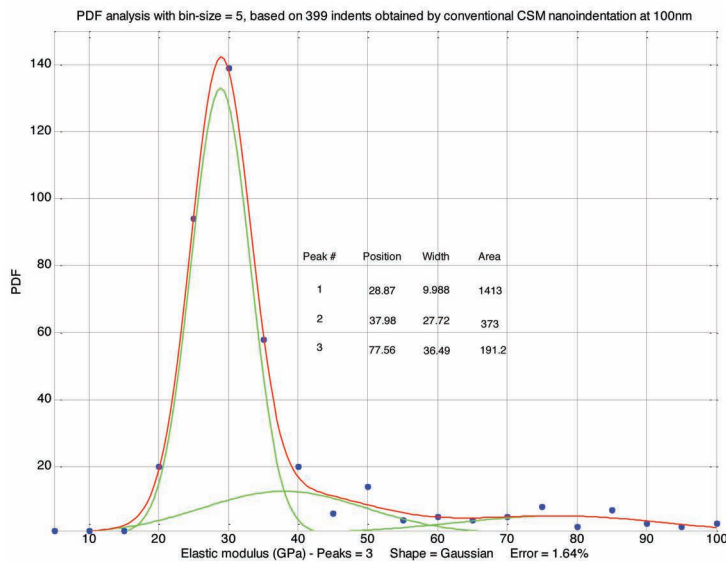
In case of the conventional map (Fig. 3a), the positions of the un-hydrated clinker grains are clearly identified, but no distinction is possible among the tri- and di-calcium silicates (C2S and C3S), the Calcium aluminate and ferrite (C3A and/or C4AF). The SEM-EDS maps reported in the Figure 2b show the presence of a C3S clinker grain (bottom right), a mixed C3S/C4AF grain (top left), a magnesium

oxide (MgO) particle (white particle) and three smaller C3S grains. The inner product of hydration (HD-CSH) is clearly recognizable as the violet (Si-rich) crown around the un-hydrated C3S grains. The LD-CSH (Ca-rich) is the light blue matrix. The elemental distribution in the EDS maps was not observed previously.

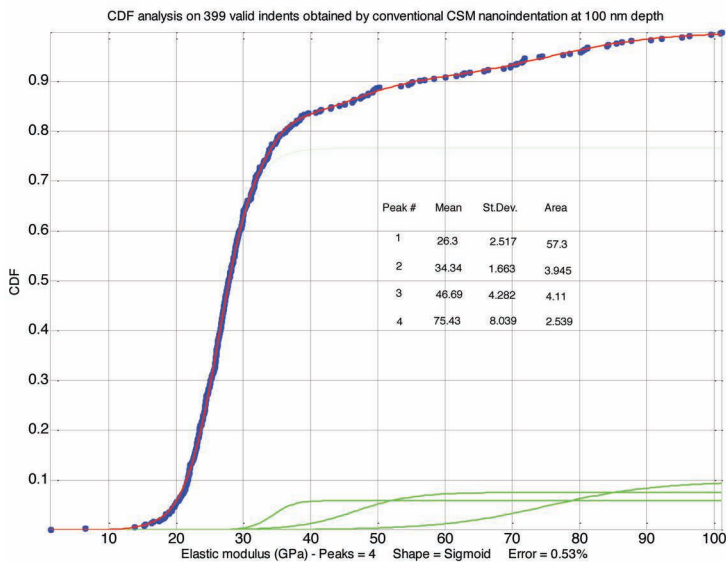
In contrast with the conventional low-resolution maps, an almost perfect correspondence is noticed between the mechanical maps (Fig. 4a-b) and the SEM-EDS map (Fig. 4c) when using

the express test. Also in this case, C3S, mixed C3S/C4AF and MgO particles are identified by EDS analysis (Fig. 4c). Those particles are all clearly defined by the Express Test mapping, where the elastic modulus gradients inside single phases are also well-defined. In particular, higher modulus is found for the C4AF and MgO grains with respect to the C3S clinker grains. Clear distinctions in terms of hardness are also observed.

EDS maps showed a higher Si/Ca ratio for the HD-CSH, even though a more



a



b

Figure 5. (a) Gaussian Distribution (PDF) analysis with bin-size = 5 GPa, based on 399 indents obtained by the conventional CSM method at 100 nm depth (b) Cumulative Distribution Function (CDF) analysis on 399 indents obtained by the conventional CSM method at 100 nm depth.

homogeneous Si distribution is observed on this area. The two C-S-H phases identified (LD, HD-CSH), corresponds to two different packaging densities of the basic building block. This suggest that the local Si ion mobility could be reduced in correspondence of the clinker/matrix interface so to give a Si-rich phase.

It is important to note that the Elastic Modulus map obtained by ultra-fast indentation is also able to identify the LD and HD-CSH phases directly on the map.

The use of the ultra-fast nanoindentation approach is a real enabling technology for this application, as it allows to achieve real micron-scale spatial resolution for mechanical property mapping.

This is further confirmed by the statistical deconvolution analysis reported in the Figures 5 and 6. On one hand, deconvolution from 399 valid conventional tests gives unstable results when using the PDF approach for data analysis.

In fact, a significant effect of the adopted bin-size on the results was observed when using the PDF approach: this is clearly due to the low peak intensity for the secondary phases, which is of the same order (or even lower) than the average noise associated to the experiments (roughness and other edge effects). The example reported in the Figure 5a is the one which gives the lowest fitting error.

Note that previous literature studies report extremely similar data [5], thus meaning that quantitative evaluation of the secondary phases is very difficult by using a conventional nanoindentation approach, or at least it is strongly affected by the noise associated to measurements.

On the other hand, the analysis of 33134 valid tests obtained by the Express Test method give extremely robust results irrespective of the adopted deconvolution approach (PDF and CDF):

in all cases, peaks corresponding to the four main phases are identified in a reproducible way, being ALL peak intensity significantly higher than the noise associated to measurements. So, the most reliable mechanical properties of the cement paste are those given in the Figure 4a–b: four main phases are identified, namely the LD-CSH, HD-CSH and two peaks corresponding to the two main un-hydrated clinker grains (C3S and C4AF).

Finally, it is interesting to make a quantitative comparison between the average elastic moduli of the hydrated phases, as obtained by the conventional and Express Test methods.

As reported in Figures 5–6, the Express Test seems to overestimate the elastic modulus of the CSH phases, in comparison with the conventional nanoindentation.

This is likely due to the significant strain-rate sensitivity of cement-based materials, which was already reported in previous papers. The higher elastic moduli obtained by the express test are then simply related to the higher strain-rate during testing.

Conclusion

In this work, the hydration mechanisms of a commercial cement paste have been investigated by the use of an innovative statistical ultra-fast nanoindentation method.

The two-dimensional analysis of mechanical phases, coupled with SEM-EDS maps, revealed the presence of two distinct hydrated phases (low density and high-density CSH). High-density and low-density phases correspond to the inner and outer products of hydration, respectively. By correlation with SEM-EDS observations, different packing densities were also correlated to different Si/Ca ratios. Gradients of elastic modulus inside the clinker grains are also resolved by this method.

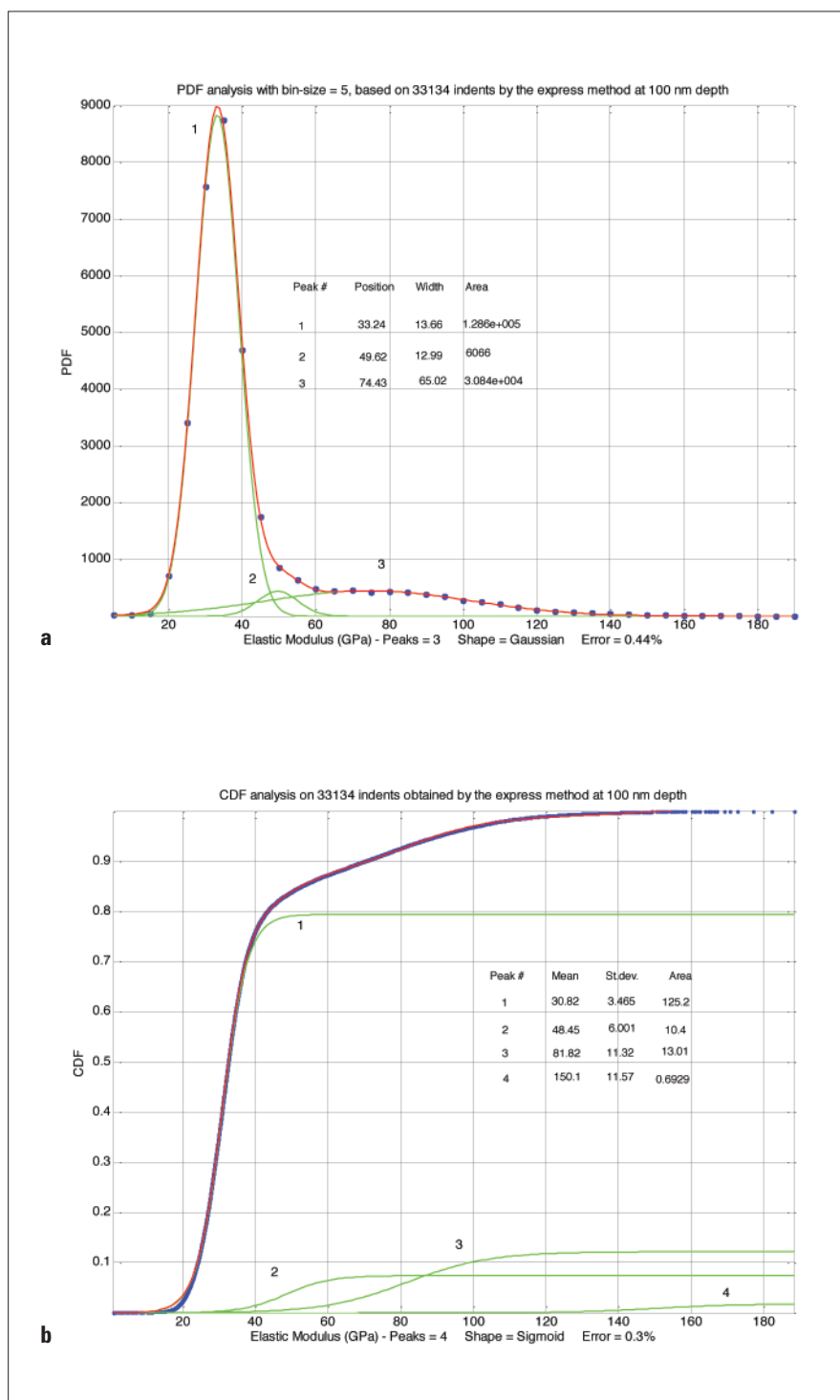


Figure 6. (a) Gaussian Distribution (PDF) analysis with bin-size = 5, based on 33134 indents by the express method at 100 nm depth (b) Cumulative Distribution Function (CDF) analysis on 33134 indents obtained by the express method at 100 nm depth.

The adopted ultra-fast indentation method also allows to distinguish between the different phases that are present inside single grains of un-hydrated phases. This gives unprecedented resolution in mapping the mechanical properties of

cement, if compared to conventional nanoindentation mapping. This experimental tool can be an enabling technology for the design of innovative cement formulations, e.g. by tailoring the relative content of the constituents and/or addition of nano-additives.

References

- [1]. H.F.W. Taylor, Cement Chemistry, Harold F.W. Taylor, ACADEMIC PRESS, London, 1990
- [2]. J.Lee, S. Mahendra, P.J.J. Alvarez, ACS nano VOL. 4, NO. 7, 2010
- [3]. Constantinides, G., Ulm, F.-J., "The effect of two types of C-S-H on the elasticity of cement-based materials: Results from nanoindentation and micromechanical modeling", 2004, Cement and Concrete Research, 34, 1, 67, 80, 214
- [4]. Velez, K., Maximilien, S., Damidot, D., Fantozzi, G., Sorrentino, F., Determination by nanoindentation of elastic modulus and hardness of pure constituents of Portland cement clinker, 2001, Cement and Concrete Research, 31, 4, 555, 561, 112
- [5]. Jennings, H.M., Thomas, J.J., Gevrenov, J.S., Constantinides, G., Ulm, F.-J., A multi-technique investigation of the nanoporosity of cement paste, 2007, Cement and Concrete Research, 37, 3, 329, 336, 88
- [6]. Constantinides, G., Ulm, F.-J., Van Vliet, K., On the use of nanoindentation for cementitious materials, 2003, Materials and Structures/Materiaux et Constructions, 36, 257, 191, 196, 82
- [7]. Ulm, F.-J., Constantinides, G., Heukamp, F.H., Is concrete a poromechanics material? - A multiscale investigation of poroelastic properties, 2004, Materials and Structures/Materiaux et Constructions, 37, 265, 43, 58, 78
- [8]. Ulm, F.-J., Vandamme, M., Bobko, C., Alberto Ortega, J., Tai, K., Ortiz, C., Statistical indentation techniques for hydrated nanocomposites: Concrete, bone, and shale, 2007, Journal of the American Ceramic Society, 90, 9, 2677, 2692, 68
- [9]. Sorelli, L., Constantinides, G., Ulm, F.-J., Toutlemonde, F., The nano-mechanical signature of Ultra High Performance Concrete by statistical nanoindentation techniques, 2008, Cement and Concrete Research, 38, 12, 1447, 1456, 51
- [10]. Mondai, P., Shah, S.R., Marks, L.D., Nanoscale characterization of cementitious materials, 2008, ACI Materials Journal, 105, 2, 174, 179, 47
- [11]. Plassard, C., Lesniewska, E., Pochard, I., Nonat, A., Investigation of the surface structure and elastic properties of calcium silicate hydrates at the nanoscale, 2004, Ultramicroscopy, 100, 3-4, 331, 338, 46
- [12]. Mondal, P., Shah, S.P., Marks, L., A reliable technique to determine the local mechanical properties at the nanoscale for cementitious materials, 2007, Cement and Concrete Research, 37, 10, 1440, 1444, 44
- [13]. Vandamme, M., Ulm, F.-J., Nanogranular origin of concrete creep, 2009, Proceedings of the National Academy of Sciences of the United States of America, 106, 26, 10552, 10557, 39
- [14]. Miller, M., Bobko, C., Vandamme, M., Ulm, F.-J., Surface roughness criteria for cement paste nanoindentation, 2008, Cement and Concrete Research, 38, 4, 467, 476, 38
- [15]. DeJong, M.J., Ulm, F.-J., The nanogranular behavior of C-S-H at elevated temperatures (up to 700°C), 2007, Cement and Concrete Research, 37, 1, 1, 12, 38
- [16]. Vandamme, M., Ulm, F.-J., Fonollosa, P., Nanogranular packing of C-S-H at substoichiometric conditions, 2010, Cement and Concrete Research, 40, 1, 14, 26

- [17]. Hughes, J.J., Trtik, P., Micro-mechanical properties of cement paste measured by depth-sensing nanoindentation: A preliminary correlation of physical properties with phase type, 2004, *Materials Characterization*, 53, 2–4, 223, 231, 35
- [18]. Zhu, W., Hughes, J.J., Bicanic, N., Pearce, C.J., Nanoindentation mapping of mechanical properties of cement paste and natural rocks, 2007, *Materials Characterization*, 58, 11–12 SPEC. ISS., 1189, 1198, 33
- [19]. Trtik, P., Münch, B., Lura, P., A critical examination of statistical nanoindentation on model materials and hardened cement pastes based on virtual experiments, 2009, *Cement and Concrete Composites*, 31, 10, 705, 714, 26
- [20]. Chen, J.J., Sorelli, L., Vandamme, M., Ulm, F.-J., Chanvillard, G., A coupled nanoindentation/SEM-EDS study on low water/cement ratio portland cement paste: Evidence for C-S-H/Ca(OH)₂ nanocomposites, 2010, *Journal of the American Ceramic Society*, 93, 5, 1484, 1493, 22
- [21]. Randall, N.X., Vandamme, M., Ulm, F.-J., Nanoindentation analysis as a two-dimensional tool for mapping the mechanical properties of complex surfaces, 2009, *Journal of Materials Research*, 24, 3, 679, 690, 19
- [22]. Vandamme, M., Ulm, F.-J., Nanoindentation investigation of creep properties of calcium silicate hydrates, 2013, *Cement and Concrete Research*, 52, 38, 52
- [23]. Da Silva, W.R.L., Nemecek, J., Štemberk, P., Application of multiscale elastic homogenization based on nanoindentation for high performance concrete, 2013, *Advances in Engineering Software*, 62–63, 109, 118

Nanomeasurement Systems from Agilent Technologies

Agilent Technologies, the premier measurement company, offers high-precision, modular nanomeasurement solutions for research, industry, and education. Exceptional worldwide support is provided by experienced application scientists and technical service personnel. Agilent's leading-edge R&D laboratories ensure the continued, timely introduction and optimization of innovative, easy-to-use nanomeasure system technologies.

www.agilent.com/find/nano

Americas

Canada	(877) 894 4414
Latin America	305 269 7500
United States	(800) 829 4444

Asia Pacific

Australia	1 800 629 485
China	800 810 0189
Hong Kong	800 938 693
India	1 800 112 929
Japan	0120 (421) 345
Korea	080 769 0800
Malaysia	1 800 888 848
Singapore	1 800 375 8100
Taiwan	0800 047 866
Thailand	1 800 226 008

Europe & Middle East

Austria	43 (0) 1 360 277 1571
Belgium	32 (0) 2 404 93 40
Denmark	45 70 13 15 15
Finland	358 (0) 10 855 2100
France	0825 010 700*
	*0.125 €/minute
Germany	49 (0) 7031 464 6333
Ireland	1890 924 204
Israel	972-3-9288-504/544
Italy	39 02 92 60 8484
Netherlands	31 (0) 20 547 2111
Spain	34 (91) 631 3300
Sweden	0200-88 22 55
Switzerland	0800 80 53 53
United Kingdom	44 (0) 118 9276201

Other European Countries:

www.agilent.com/find/contactus

Product specifications and descriptions in this document subject to change without notice.

© Agilent Technologies, Inc. 2013
Published in USA, October 15, 2013
5991-3389EN



Agilent Technologies